Supporting Information

Self-healing and Efficient Flexible Perovskite Solar Cells Enabling by Host-Guest Interaction and 2D/3D Heterostructure

Zhengchi Yang,[a] Yue Jiang, [a*] Dongdong Xu, [a] Zhen Wang, [a] Xingsen Gao [a], Xubing Lu [a], Guofu Zhou, [a, b] Jun-Ming Liu, [a, c] Jinwei Gao [a*]

a. Institute for Advanced Materials and Guangdong Provincial Key Laboratory of Optical Information Materials and Technology, South China Academy of Advanced Optoelectronics, South China Normal University, Guangzhou 510006, China.
b. Institute of Electronic Paper Displays, South China Academy of Advanced Optoelectronics, South China Normal University, Guangzhou 510006, China.
c. Laboratory of Solid-State Microstructures, Nanjing University, Nanjing 210093, China.

E-mail: gaojinwei@m.scnu.edu.cn (J.G.), yuejiang@m.scnu.edu.cn (Y.J.)

Content of the supporting information:

4. Tables

1. Experimental section

1.1 Materials

Methylammonium bromide (MABr, 99.5%), cesium iodide (CsI, 99.99%) and methylammonium chloride (MACl 99.5%) were purchased from Xi'an Polymer Light Technology Corp. Lead iodide (PbI_2, 99.999%), formamidinium iodide (FAI, 99.9%), 2,2′,7,7′-tetrakis(N,N-di-p-methoxyphenylamine)-9,9-spirobifluorene(Spiro-OMeTAD, 99.8%) and fluorine-doped tin oxide glasses(FTO, 7 Ω/sq) were purchased from Yingkou You Xuan Trade Co.Ltd. Bis(trifluoromethanesulfonyl)imide (Li-TFSI, 99.5%), tert-butylpyridine (t-BP, 98%), stannous chloride dihydrate (SnCl2·2H2O,99.99%), potassium chloride (KCl, 99.999%) dimethyl formamide (DMF, 99.8%), and dimethyl sulfoxide (DMSO, 99.9%) were purchased from Sigma–Aldrich. Chlorobenzene (CB, 99.5%), β-Cyclodextrin (β-CD, 98%), glycidyl methacrylate (GMA, 97%), 1,8-Diazabicyclo[5.4.0]undec-7-ene (DBU, 99%), 1-adamantylamine(AA, 98%), acryloyl chloride (AC, 96%), triethylamine (99%), guanidine hydrochloride (GUA, 99%), methyl methacrylate (MMA, 99%), and 2,2'-Azobis(2-methylpropionamidine) dihydrochloride (ABAP, 97%) were purchased from Shanghai Aladdin Biochemical Technology Co., Ltd.

1.2 Synthesis of Methacrylguanidine Hydrochloride (MAGH)

The synthetic scheme of MAGH was shown in **Figure S1**, and the specific method was as follows. First, guanidine hydrochloride (1.94 g, 20 mmol) was added to a solution of NaOH (0.83 g, 20 mmol) in ethanol (10 mL) and the solution was stirred under an ice bath for 3 hours. The guanidine solution was then filtered and the ethanol was distilled off using a rotary evaporator. The residue was dried in a vacuum chamber to obtain solid guanidine (1.13 g, 96% yield). Second, guanidine (0.59 g, 10 mmol) was dissolved in 7.5 ml acetone. Then MMA (1.27 mL, 12 mmol) was dropped into the guanidine solution and stirred at room temperature for 3 hours. At the end of the reaction, the cyclic by-products were filtered off. The filtrate was cooled to 0-5 °C, and then 0.83 ml of 36% hydrochloric acid was added dropwise. The mixture was stirred at room temperature for 2 h, filtered, recrystallized from acetone, and dried under vacuum

at 40 °C to obtain MAGH (0.75 g, 46%) as a white solid.

1.3 Synthesis of Glycidyl Methacrylate-Bonded β-Cyclodextrin (GMA-CD)

GMA-CD was synthesized according to previously described procedures. As shown in **Figure S2**, firstly, dry β-CD (1.157 g, 1 mmol) was dissolved in 5 mL of anhydrous DMF under N_2 atmosphere. DBU (10 μL, 0.067 mmol) and GMA (167 μL, 1.25 mmol) were then quickly added to the β-CD solution. The reaction mixture was stirred at 100 °C for 150 minutes. After the reaction was completed, the solution was cooled to room temperature and filtered to remove insoluble by-products. Next, the filtrate was added dropwise to 50 mL of toluene to form a precipitate, which was filtered and washed with 30 mL of toluene and acetone, respectively. Finally, it was dried in a vacuum oven at 40 °C for 12 h to obtain GMA-CD (1.277 g, 95% yield).

1.4 Synthesis of N-adamantylacrylamide (N-AA)

As shown in **Figure S3**, amantadine (4 mmol, 0.62 g) was dissolved in 50 mL of tetrahydrofuran (THF) at 60 °C, and the solution was cooled to 0-5 °C. Trimethylamine (0.63 mL, 2.8 mmol) was added to the solution and stirred for 30 minutes, then acryloyl chloride (0.31 mL, 4.8 mmol) in 20 mL of THF was added dropwise to the solution. The solution was stirred in an ice-water bath for 6 hours. The precipitate was removed by suction filtration, and the solvent in the filtrate was removed by rotary evaporation to obtain a yellow solid. It was purified by silica gel column chromatography (ethyl acetate/petroleum ether = 3/7) and recrystallized from methanol to obtain colorless transparent crystals, namely N-AA (0.4 g, yield 49%)

1.5 Synthesis of MAGH/GMA-CD/N-AA Terpolymer (P(MAGH-CD-AA))

The P(MAGH-CD-AA) was synthesized as follows. A mixture of MAGH (1.64 g, 10 mmol), GMA-CD (0.13 g, 0.1 mmol), N-AA (0.021 g, 0.1 mmol), ABAP (10 mg), DMF (8 mL) and DMSO (2 mL) was added to a 50 mL round bottom flask. Under nitrogen protection, the mixture was stirred at 65 °C for 1 h, and then the mixture was

poured into a 5 mm (diameter) × 120 mm (length) glass tube or a square mold of 80 mm×10 mm×4 mm. Polymerization was carried out at 65°C overnight to obtain P(MAGH-CD-AA). GPC (Mp = 35431, Mn = 30908, Mw = 36151, Mz = 42103, Mz+1 = 49257, PD = 1.17)

1.6 Preparation of Colloidal SnO_2 NCs Solution

SnO_2 NCs solutions were prepared using our previous methods. Briefly, a certain amount of $SnCl_2{\cdot}2H_2O$ was dissolved in a water-butanol solution. The $SnCl_2{\cdot}2H_2O$ solution was then refluxed at 110° C for 2-4 hours.

1.7 Preparation of Perovskite Precursor Solution

The 1.52 M $Cs_{0.05}(MA_{0.11}FA_{0.89})_{0.95}Pb(I_{0.97}Br_{0.03})_3$ perovskite precursor solution was prepared by mixing PbI_2 (5% molar excess of PbI_2) FAI, MABr, MACl, and CsI in component solvent (DMF/DMSO=4/1). The MAGH, GMA-CD, N-AA and MAGH/GMA-CD/N-AA tertiary prepolymer (TPP, molar ratio 100/1/1) solutions were prepared by dissolved a certain mass of MAGH, GMA-CD, N-AA and TPP in component solvent (DMF/DMSO=4/1), separately. For MAGH, GMA-CD, N-AA, or TPP -doped perovskite precursor solutions at concentrations ranging from 0.01-5 $mg{\cdot}mL^{-1}$, their solutions were added to the control perovskite precursor solution.

1.8 Device Fabrication

The FTO substrates were sequentially ultrasonically washed with detergent, deionized water, and isopropanol for 15 minutes, and then UV ozone treated for 15 minutes before use. SnO_2 NCs were spin-coated onto FTO substrates at 3000 rpm for 30 s in ambient air. After the FTO/SnO_2 substrates were annealed at 150 °C for 30 min, 10 mM KCl aqueous solution was spin-coated for 30 s at 3000 rpm and annealed at 100 °C for 10 min. All SnO_2 layers were treated equally with aqueous KCl, attributed to reduced hysteresis, interfacial recombination and improved luminescence. Before perovskite deposition, the FTO/SnO_2 substrate was UV ozone treated and put into a nitrogen glove.

The perovskite precursor solution was spin-coated on SnO_2 layer by two-consecutive step program at 1000 rpm for 10 s with a ramping rate of 500 rpm, and 5000 rpm for 30 s with a ramping rate of 1000 rpm. During the second step, 100 μL of CB was poured on the center of the spinning substrates 10 s prior to the end of spinning program, followed by annealing at 100 °C for 1h on the heating stage.

20 μL of spiro-OMeTAD solution, dissolved 72.3 mg of spiro-OMeTAD, 17.5 μL of Li-TFSI solution (520 mg in 1 mL acetonitrile) and 28.8 μL of t-BP in 1 mL CB, was spin-coated upon perovskite layer at 500 rpm for 3 s, and 3000 rpm for 30 s. Finally, the Ag electrode (100 nm) was fabricated by thermal evaporation, and the effective area of all devices was 0.07 cm^2 defined as a metal mask.

2. Characterization

2.1 Fourier Transform NMR Spectroscopy

1 H NMR and 13 C NMR spectra were obtained on a Bruker AVANCE NEO (600 MHz) with DMSO-d6 as the solvent.

2.2 Fourier Transform infrared spectroscopy (FTIR)

The FTIR spectra were recorded by Bruker Optic Gmbh in the 4000 cm^{-1}~400 cm^{-1} range.

2.3 Gel permeation chromatography **(GPC)**

The molecular weight and polydispersity index (PD) of polymers were measured with LC20AT GPC (SHIMADZU, Japan) equipped with a RID-20A detector based on PEO standards, respectively, using ultrapure water as the eluting solvent.

2.4 Scanning electron microscopy (SEM)

The morphology and microstructures of perovskite films deposited on FTO substrates were investigated by FE-SEM (ZEISS Ultra-55).

2.5 X-ray diffraction (XRD) characterization

The crystal structure and phase of the perovskite based on different concentrations of TPP-MCDAA doped were characterized using an XRD (BRUKER D8 ADVANCE).

2.6 Ultraviolet–visible spectroscopy (UV–vis), ultraviolet photoelectron spectroscopy (UPS) and X-ray photoelectron spectroscopy (XPS)

The absorption spectra of perovskite film were measured by UV–vis spectrometer (SHIMADZU UV-2600). UPS and XPS characterizations were performed by AXIS SUPRA using perovskite films spin-coated on the glass/ITO/SnO_2 substrates.

2.7 Steady-state photoluminescence (PL) and time-resolved photoluminescence (TRPL)

PL and TRPL were measured by fluorescence spectrometers (Edinburgh Instruments F97Pro and Edinburgh Instruments FLS1000/FS5) with excitation wavelengths of 500 nm and 450 nm, respectively, using perovskite films prepared on glass.

2.8 Solar cell performance characterization

The J-V characteristics were measured with a Keithley 2440 source under a simulated AM1.5G spectrum. The EQE measurements of photovoltaic devices were carried on EQE system (Enli Technology Co., Ltd QE-C) in a wavelength range of 300–900 nm. Steady-state output of solar devices were measured under continuous illumination of AM 1.5G 100 $mW \cdot cm^{-2}$ and a constant voltage bias near the maximum power point. The constant voltages of the two perovskite devices based on the reference and TPP-MCDAA doped are 0.930 V, 0.955 V and 0.995 V, respectively.

2.9 Electrochemical impedance spectroscopy (EIS)

EIS was measured using the Zahner Zennium electrochemical workstation with a 5mV AC sinusoidal signal source in the frequency range of 10 Hz to 1.0 MHz.

Note: we mainly focus on charge transporting issues of devices based on different

antisolvents treatment and the whole arc located in higher frequency region (103~106Hz)

2.10 Space charge limited current (SCLC)

Two kind of device were fabricated with configuration of ITO/PEDOT:PSS/Perovskite/Spiro-OMeTAD/Ag for hole-only devices, and ITO/SnO_2/Perovskite/PCBM /Ag for electron-only devices. According to SCLC theory, the defect density could be obtained from the trap-filled-limited voltage (V_{TFL}) using the equation $N_t = 2\varepsilon\varepsilon_0 V_{TFL}/(eL^2)$, where ε is relative dielectric constant of perovskite and ε_0 is the vacuum permittivity, e is the elementary charge of an electron and L is the thickness of the perovskite film (600 nm). The relative dielectric constant ε of perovskite is assumed to be 32.

2.11 Atomic force microscope (AFM)

The surface roughness of perovskite films was obtained from the AFM (Asylum Research, Cypher).

3. Figures

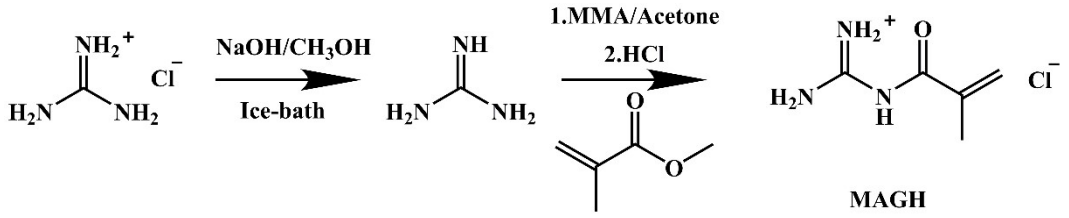

Figure S1. Synthetic scheme of MAGH.

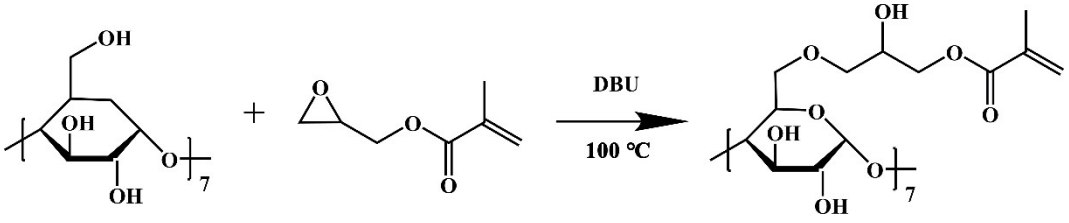

Figure S2. Synthetic scheme of GMA-CD.

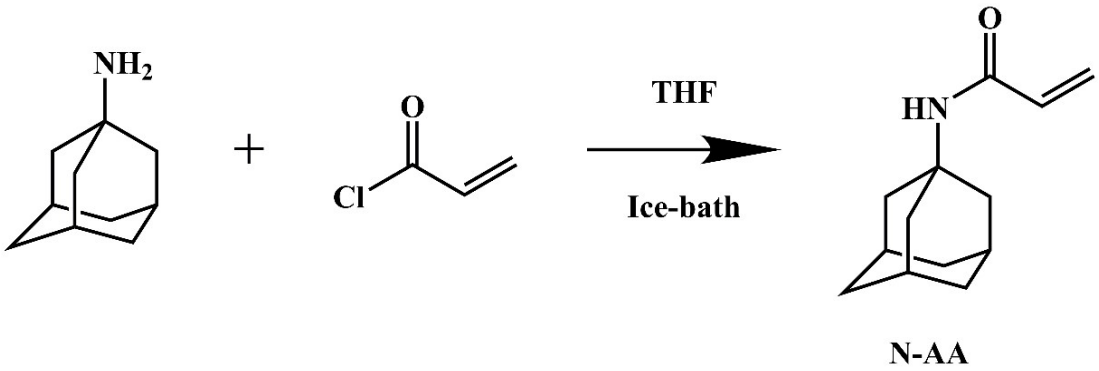

Figure S3. Synthetic scheme of N-AA.

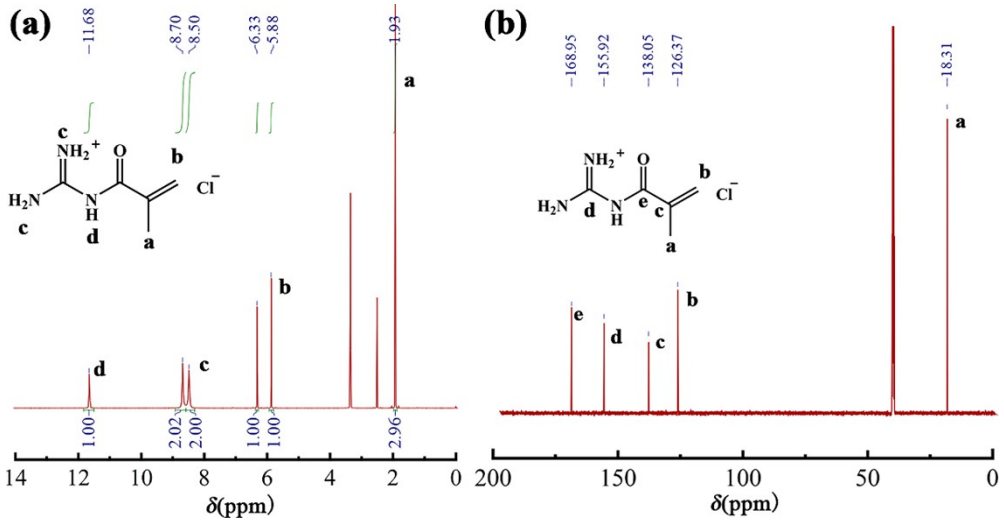

Figure S4. (a)^{1}H and (b) ^{13}C NMR spectra of MAGH.

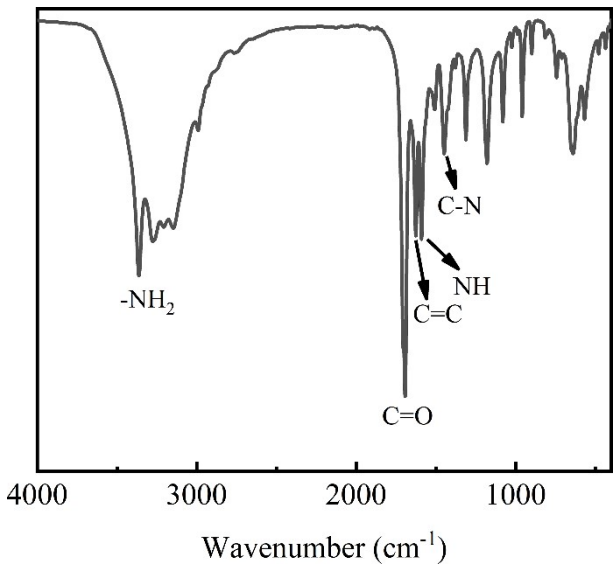

Figure S5. FT-IR spectrum of MAGH.

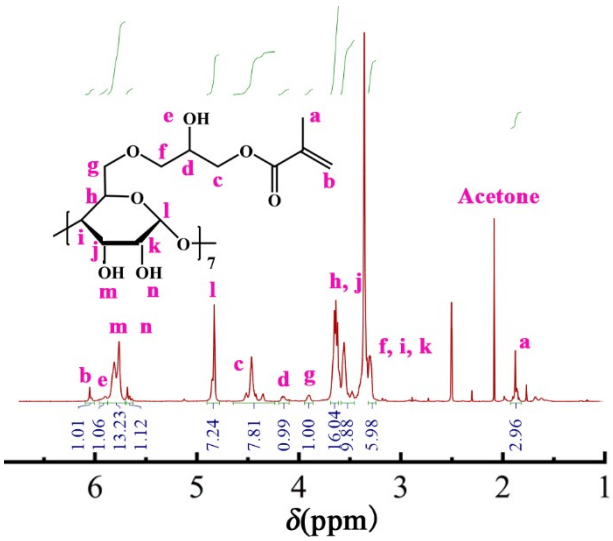

Figure S6. ^{1}H spectrum of GMA-CD.

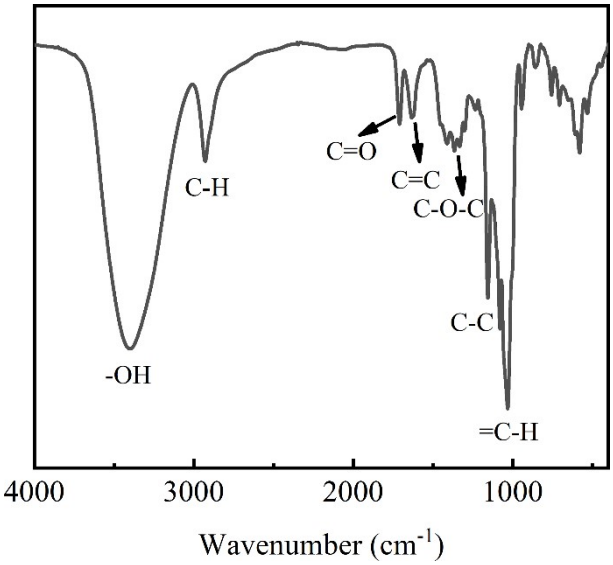

Figure S7. FT-IR spectrum of GMA-CD.

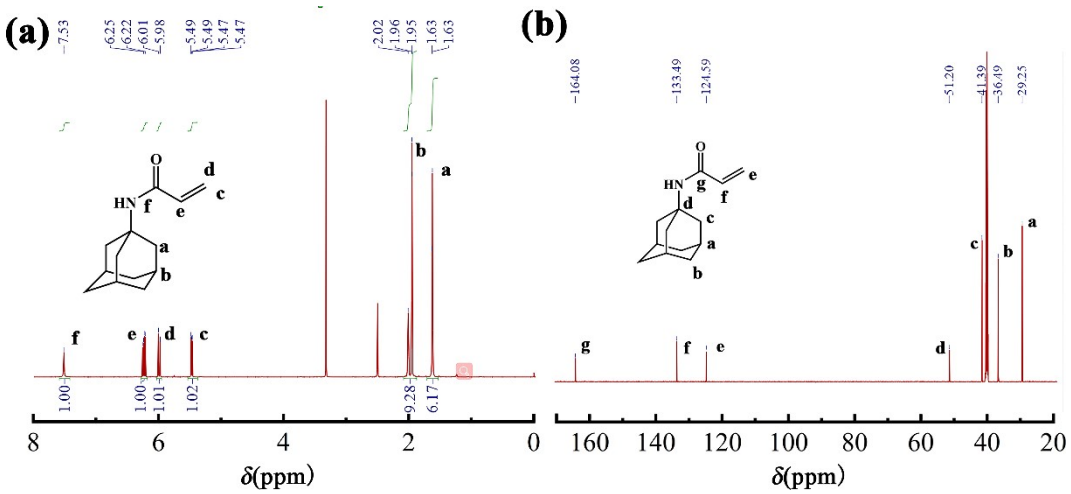

Figure S8. ^{1}H and ^{13}C NMR spectra of N-AA.

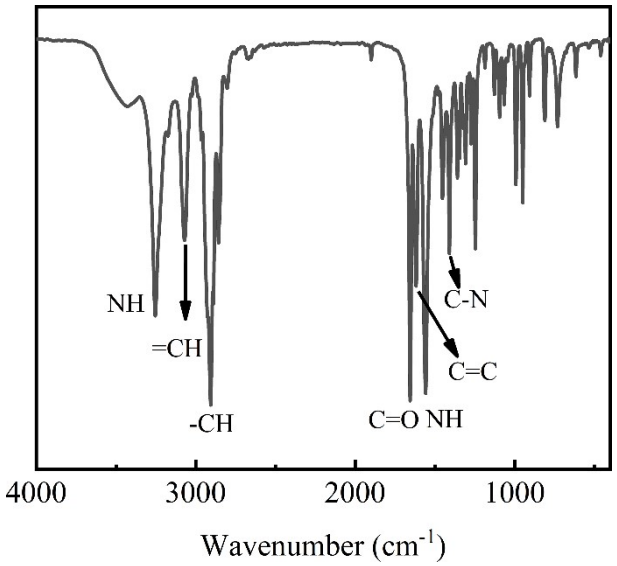

Figure S9. FT-IR spectrum of N-AA.

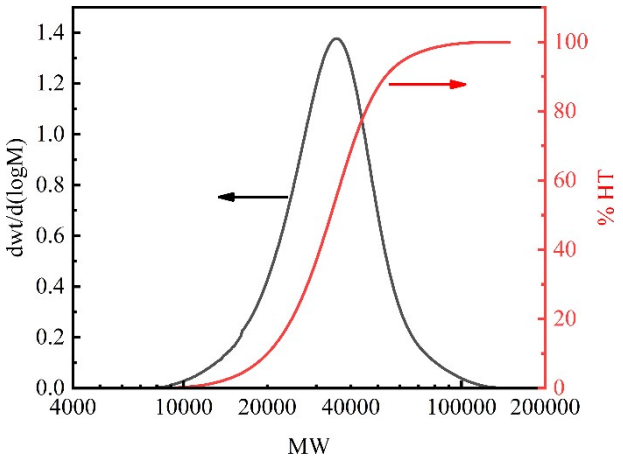

Figure S10. Molecular weight distributions of the TPP polymer.

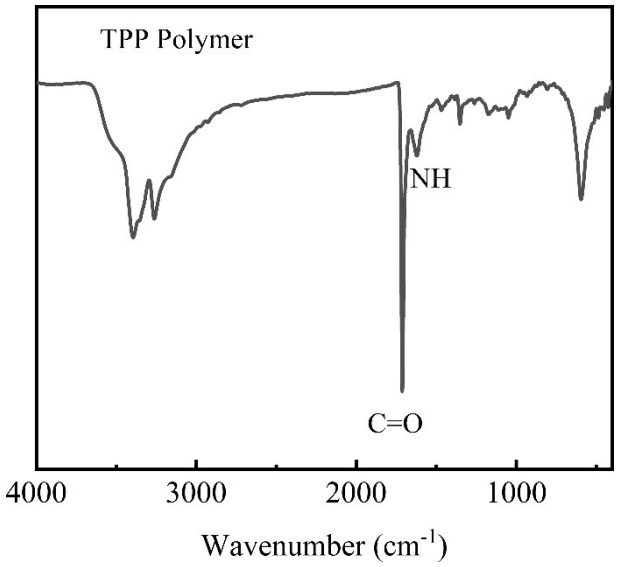

Figure S11. FT-IR spectrum of TPP polymer.

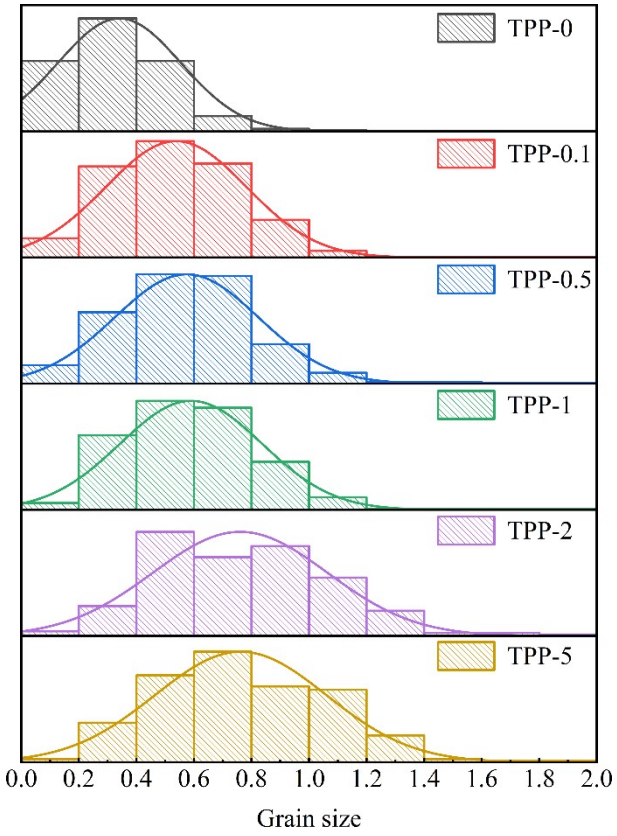

Figure S12. Grain size distribution extracted from SEM images of the Control TPP-0 and TPP-added perovskite films.

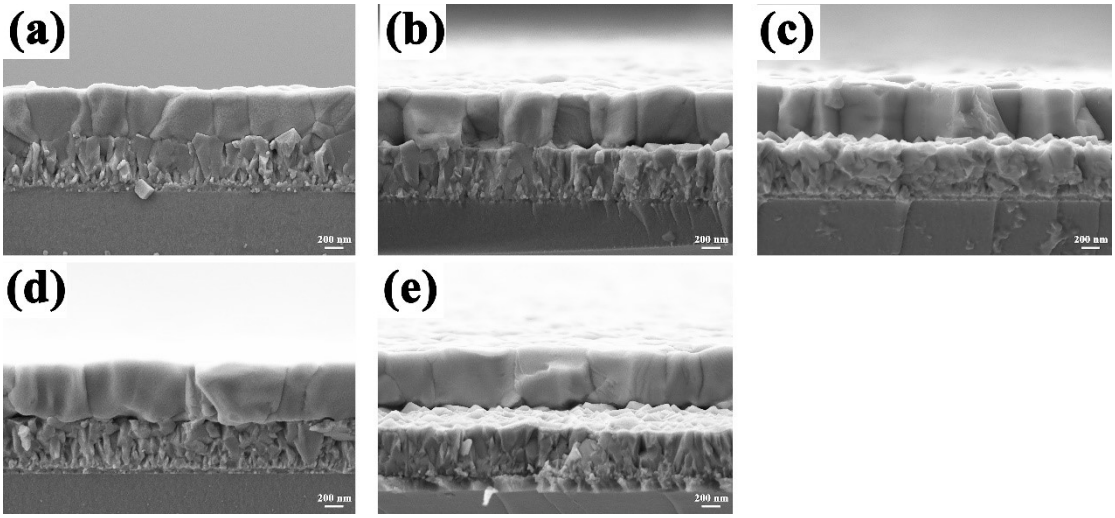

Figure S13. (a-e) Cross-sectional SEM images of **(a)** Control TPP-0, **(b)**TPP-0.1, **(c)**TPP-0.5, **(d)** TPP-1, and **(e)**TPP-2 perovskite films.

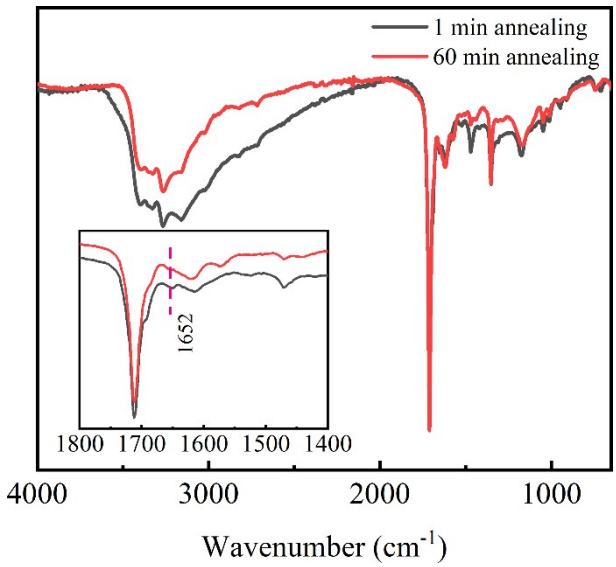

Figure S14. FT-IR spectra of TPP-added perovskite films before and after annealing

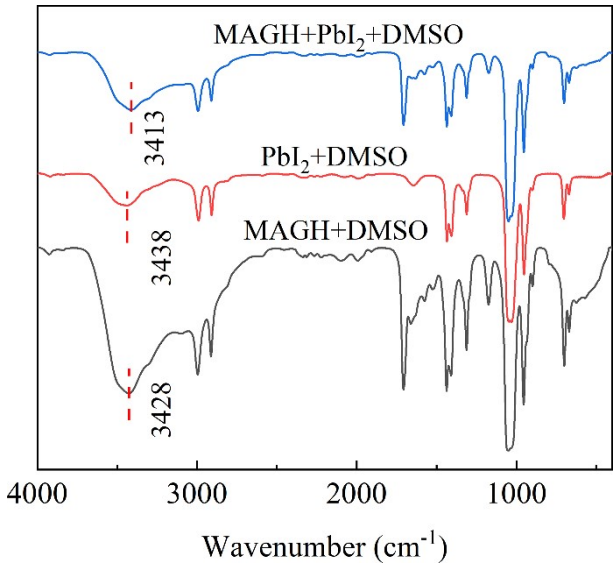

Figure S15. FT-IR spectra of the MAGH and mixed MAGH+PbI_2.

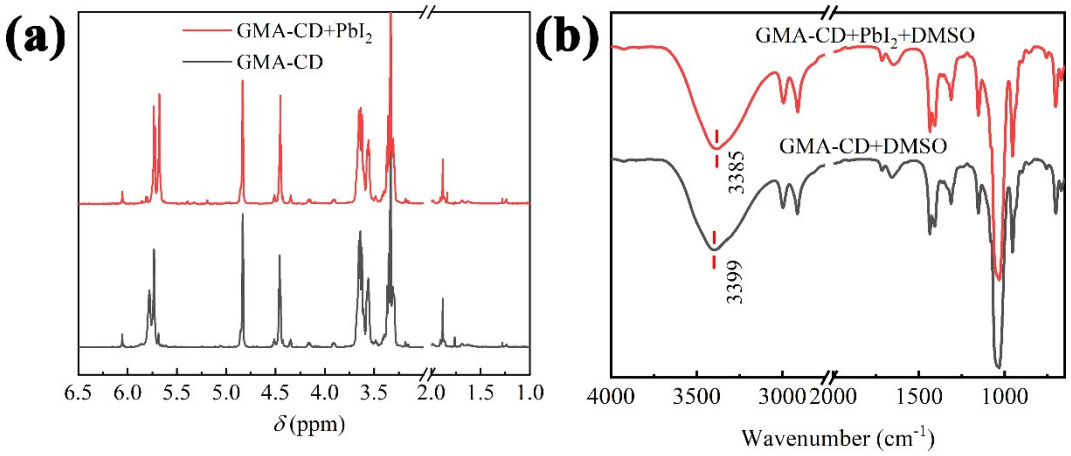

Figure S16. (a) ^{1}H NMR spectra and **(b)** FT-IR spectra of the GMA-CD and mixed GMA-CD +PbI_2.

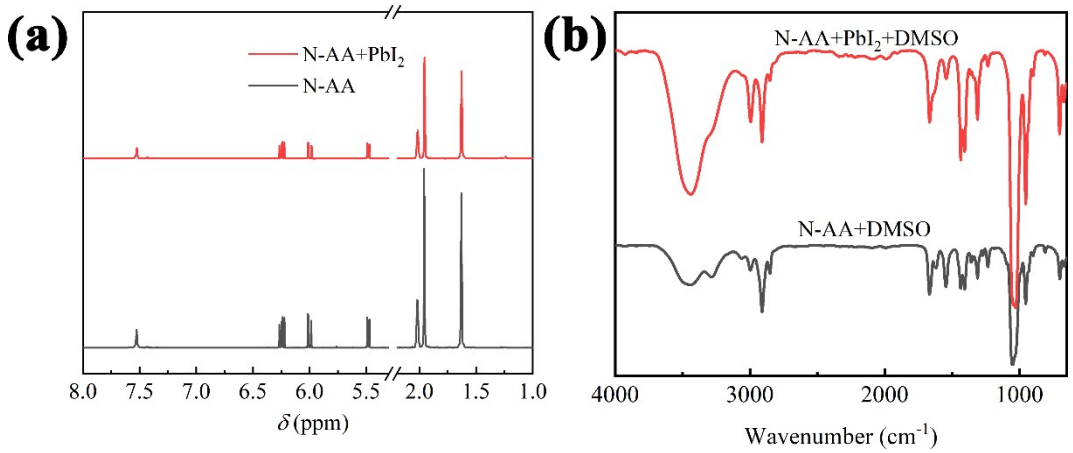

Figure S17. (a) ^{1}H NMR spectra and **(b)** FT-IR spectra of the N-AA and mixed N-AA +PbI_2.

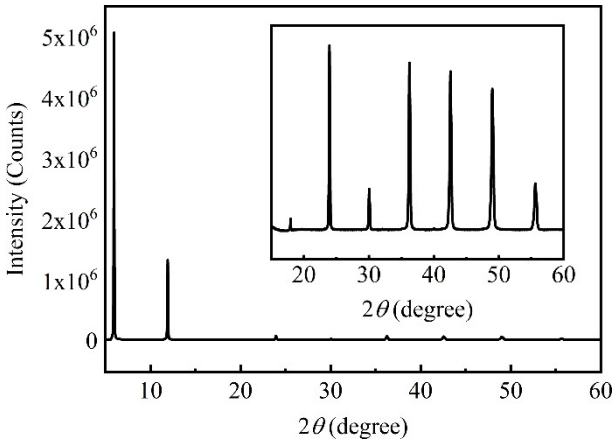

Figure S18. The XRD pattern of 2D perovskite $(MAGH)_2PbI_4$ thin films.

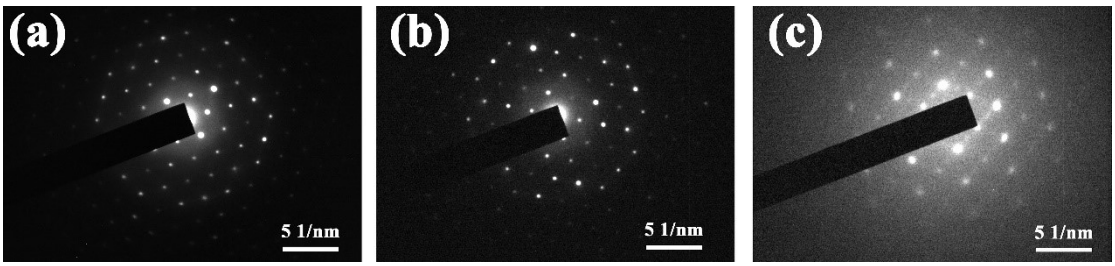

Figure S19. 3D area electron diffraction (SAED) patterns of (a) TPP-0, (b) TPP-0.5 and (c) TPP-5 perovskite films

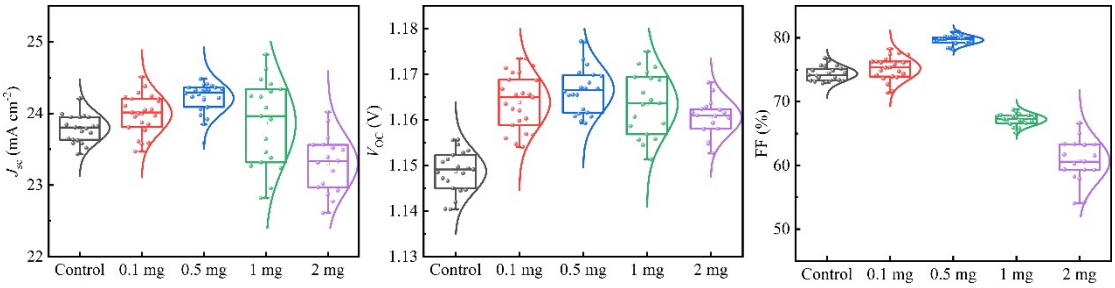

Figure S20. J_{sc}, V_{oc}, FF statistical photovoltaic data of PSCs at different MAGH concentrations.

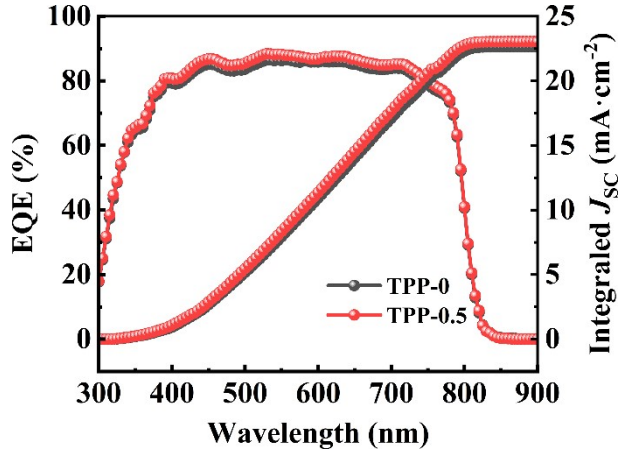

Figure S21. EQE spectra of the best performing PSCs.

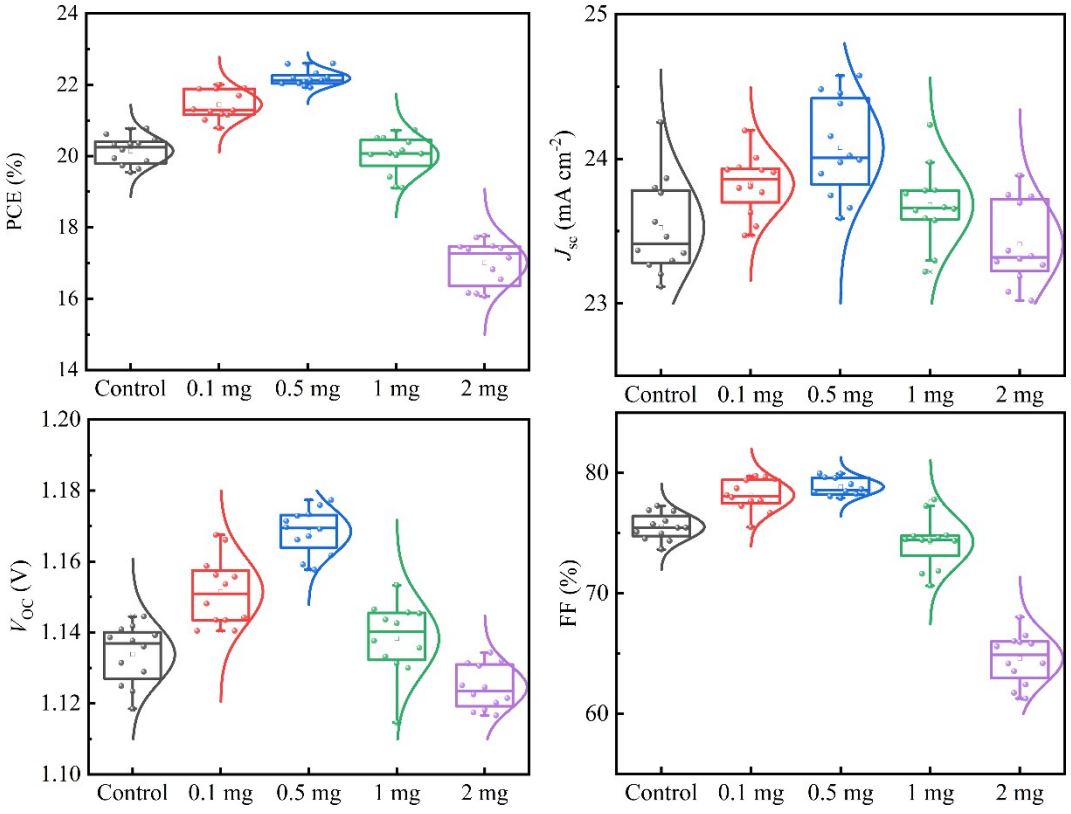

Figure S22. PCE, J_{SC}, V_{OC}, *FF* statistical photovoltaic data of PSCs at different MAGH concentrations.

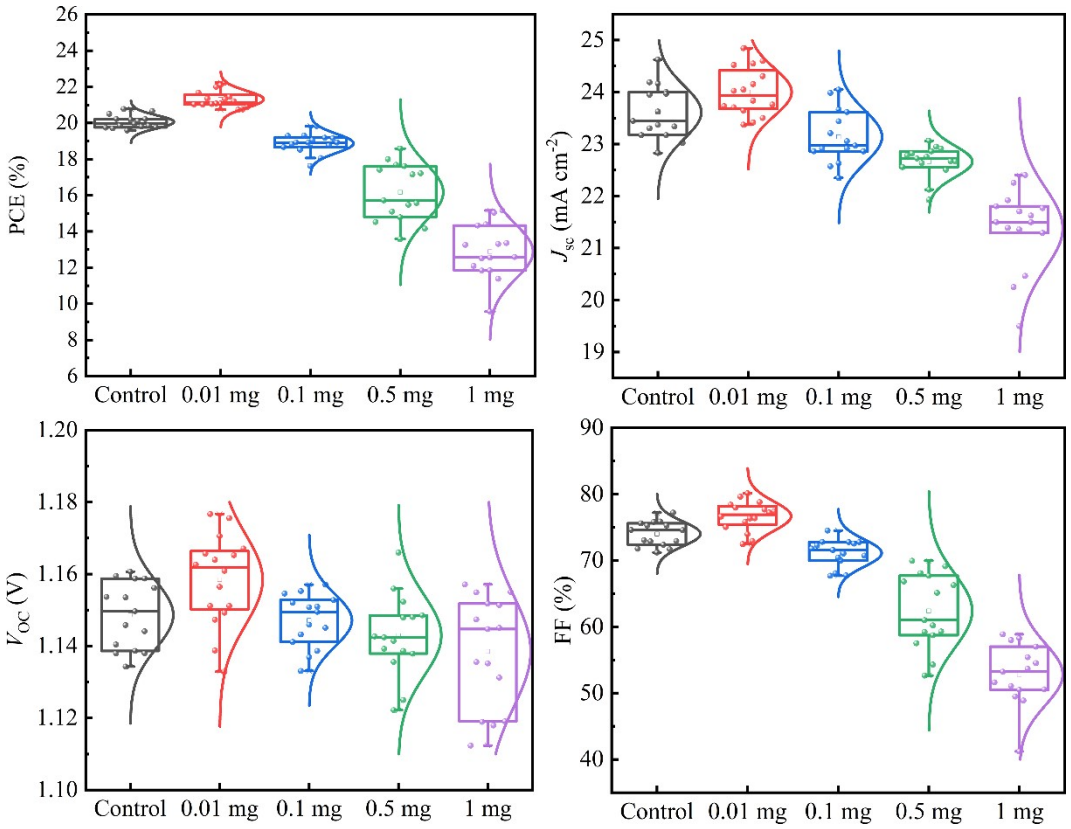

Figure S23. PCE, J_{SC}, V_{OC}, *FF* statistical photovoltaic data of PSCs at different GMA-CD concentrations.

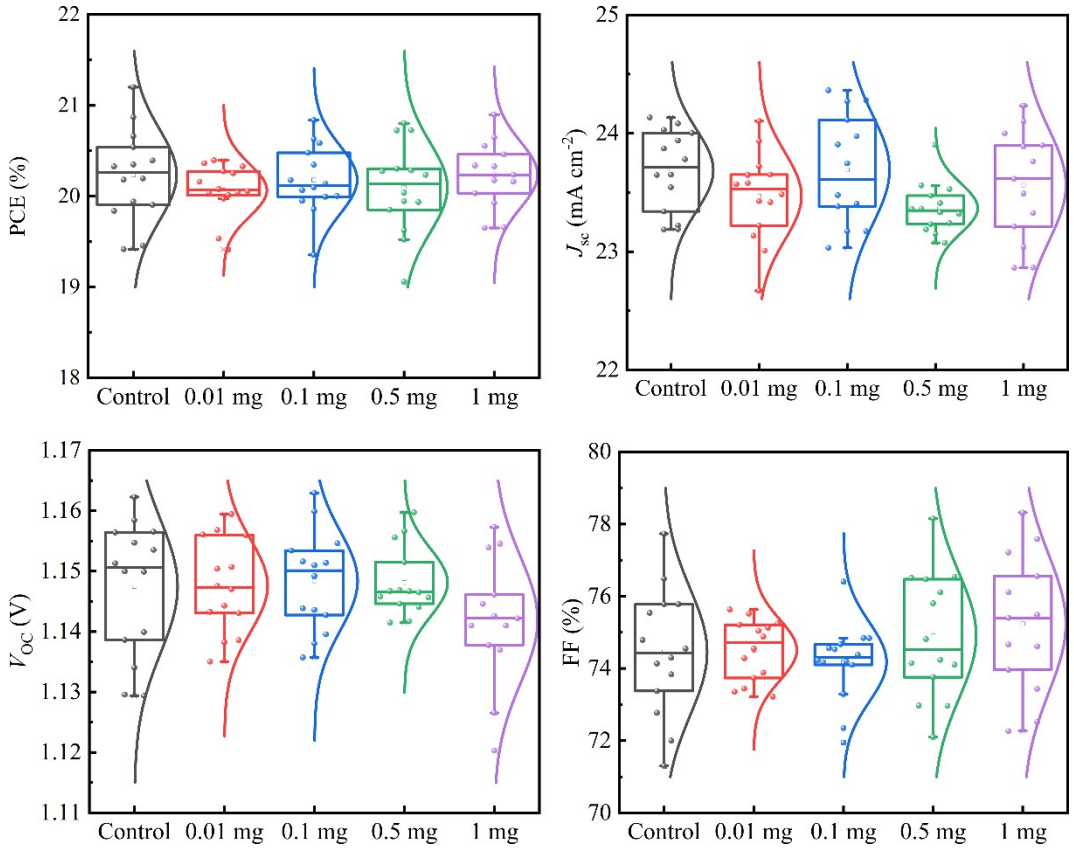

Figure S24. PCE, J_{SC}, V_{OC}, *FF* statistical photovoltaic data of PSCs at different N-AA concentrations.

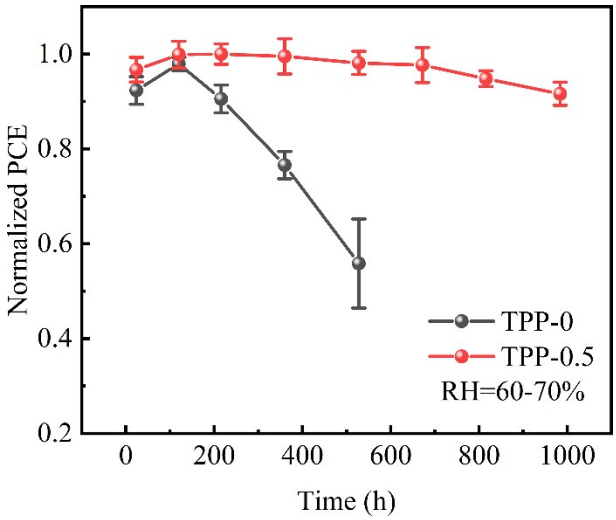

Figure S25. Long-term stability of unencapsulated PSCs storage in air (RH=60-70%).

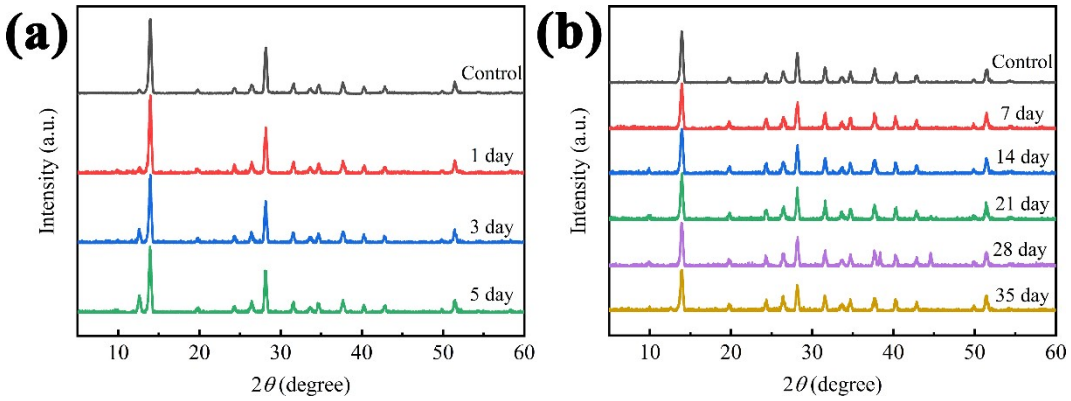

Figure S26. XRD spectra of fresh and aged perovskite films of (a) TPP-0 and (b) TPP-0.5.

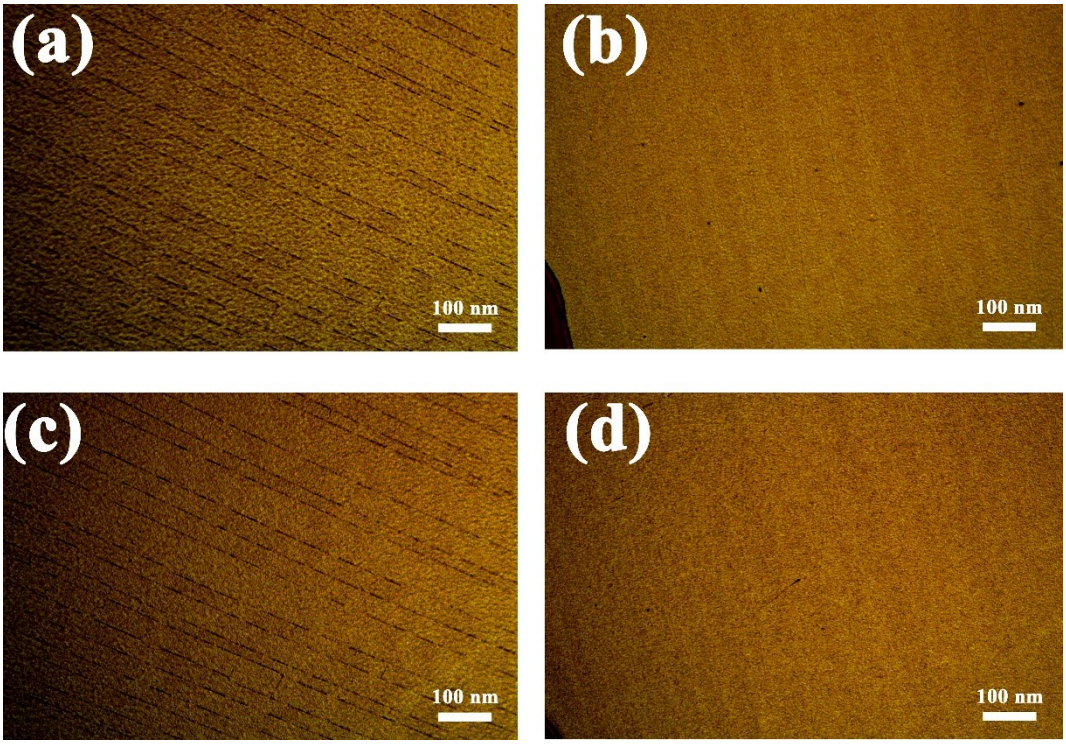

Figure S27. Optical images of control (a) TPP-0 and (b) TPP-0.5 perovskite films after 1000 bending cycles. Optical images of control (c) TPP-0 and (d) TPP-0.5 perovskite films after standing for 4 h (RH=60-70%).

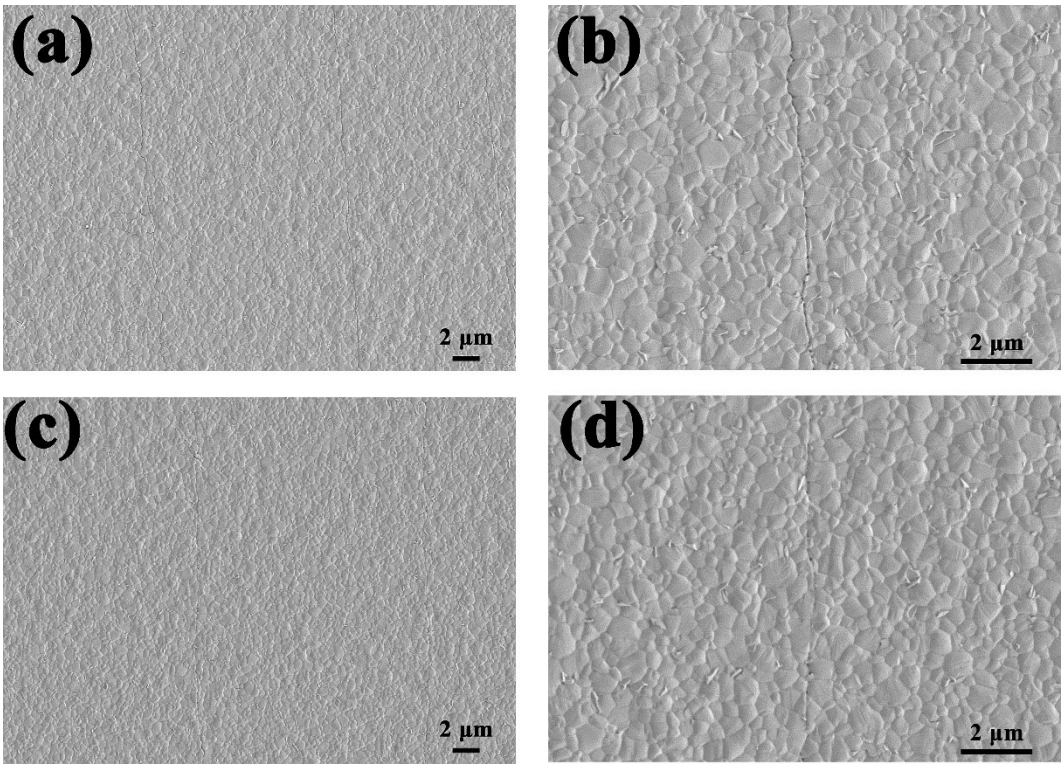

Figure S28. SEM images of control (a-b) TPP-0 and (c-d) TPP-0.5 perovskite films after 1000 bending cycles.

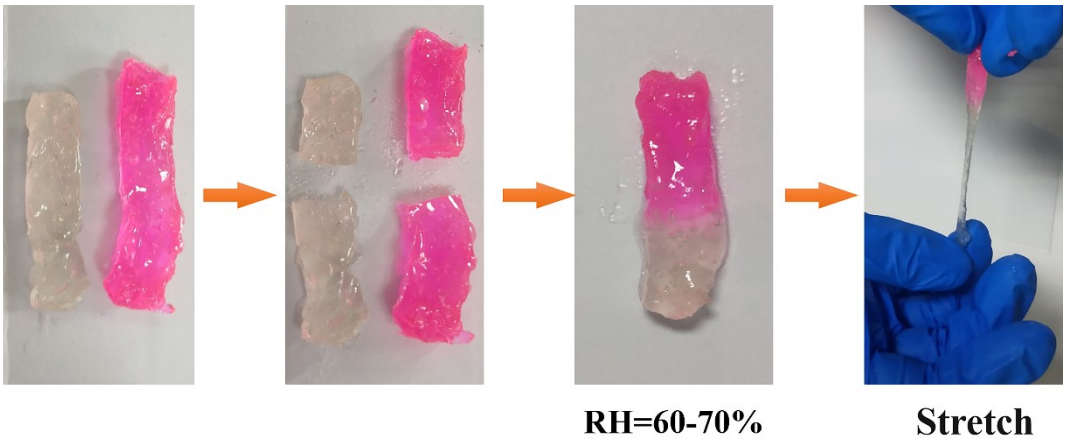

Figure S29. TPP polymers of the two slices were tightly bound together.

4. Tables

Table S1. The calculated *d*-spacing of the 2D perovskite $(MAGH)_2PbI_4$ film from XRD data.

hkl	2θ (degree)	*d* (Å)
001	5.957	14.83
002	11.918	7.41
003	17.959	4.94
004	23.948	3.71
005	30.064	2.97
006	36.281	2.47
007	42.597	2.12
008	49.048	1.86
009	55.679	1.64

Table S2. TRPL fitting results obtained for perovskite films with different amounts of TPP.

	τ_1 (ns)	A_1	τ_2 (ns)	A_2	$\tau_{average}$ (ns)
Control	68.32	945.22	210.26	956.19	175.76
0.1 mg	60.70	769.05	219.26	1068.21	192.91
0.5 mg	503.23	178.42	1810.45	924.88	1743.92
1 mg	41.73	150.30	1487.06	950.30	1480.67
2 mg	11.63	3939.82	623.45	986.06	581.00

Table S3. Optimized Photovoltaic device parameters of PSCs with different amounts of TPP

	*V*oc (V)	*J*sc (mA cm^{-2})	*FF* (%)	PCE (%)
Control	1.15	23.80	74.39	20.34
0.1 mg	1.16	24.00	75.21	21.00
0.5 mg	1.17	24.21	79.65	22.50
1 mg	1.16	23.87	67.21	18.66
2 mg	1.16	23.30	60.67	16.40

Table S4. Optimized Photovoltaic device parameters of PSCs with different amounts of MAGH.

	*V*oc (V)	*J*sc (mA cm^{-2})	*FF* (%)	PCE (%)
Control	1.13	23.53	75.53	20.15
0.1 mg	1.15	23.83	78.17	21.45
0.5 mg	1.17	24.08	78.85	22.18
1 mg	1.14	23.68	74.26	20.02
2 mg	1.12	23.41	64.61	17.01

Table S5. Optimized Photovoltaic device parameters of PSCs with different amounts of GMA-CD.

	*V*oc (V)	*J*sc (mA cm^{-2})	*FF* (%)	PCE (%)
Control	1.15	23.61	74.01	20.06
0.01 mg	1.16	24.00	76.68	21.31
0.1 mg	1.15	23.14	71.12	18.87
0.5 mg	1.14	22.66	62.40	16.17
1 mg	1.14	21.38	52.82	12.89

Table S6. Optimized Photovoltaic device parameters of PSCs with different amounts of N-AA.

	*V*oc (V)	*J*sc (mA cm^{-2})	*FF* (%)	PCE (%)
Control	1.15	23.69	74.46	20.24
0.01 mg	1.15	23.47	74.51	20.07
0.1 mg	1.15	23.69	74.18	20.18
0.5 mg	1.15	23.37	74.91	20.10
1 mg	1.14	23.56	75.24	20.24

Table S7. Survey on the application of self-healing materials in PSCs

	Self-healing material	**Self-healing mechanisms**	**Self-healing condition**	**Performance**	**Performance after healing**	**Ref.**
1	$TUEG_3$ polymer	Hydrogen bond	100 °C,1 h	6.46% PCE,	80% of initial PCE	[1]
2	Polyurethane (s-PU)	Dynamic oxime–carbamate bonds	100 °C,10 mins	19.15% PCE, 1000 cycles at 20% stretch	88% of initial PCE	[2]
3	Polyurethane (PU)	Dynamic Disulfide Bond	80 °C, 30 mins	19.15% PCE, 28 h at 50% RH and 25 °C.	90% of initial PCE	[3]

4	Poly(acrylamide - n-butyl acrylate)AD-23	Hydrogen-bond	70 °C, 5 mins	20.50% PCE, 500 cycles at bending	20.23% PCE	[4]
5	Self-healing polysiloxane (SHP)	Coordination units and hydrogen bonds	R.T., 2 h	19.50% PCE, 150 cycles at 20% stretch	80% of initial PCE	[5]
6	Fullerene derivatized polyurethane(C60-PU)	Disulfide bond	80 °C, 10 mins	21.36% PCE, 500 h at 50% RH and 25 °C	78% of initial PCE	[6]
7	Polyurethane elastomers with disulfide bonds (PUDS)	Disulfide bonds	80 °C, 10 mins	17.19% PCE, 1000 cycles at bending	88% of initial PCE	[7]
This work	**MAGH, GMA-CD and N-AA ternary prepolymer (TPP)**	**Host-guest interaction**	**60-70% RH, 4h**	**20.46% PCE, 4000 cycles at bending**	**90% of initial PCE**	

References

1. B. P. Finkenauer, Y. Gao, X. Wang, Y. Tian, Z. Wei, C. Zhu, D. J. Rokke, L. Jin, L. Meng, Y. Yang, L. Huang, K. Zhao and L. Dou, *Cell Rep. Phys. Sci.*, 2021, **2**, 100320.
2. X. Meng, Z. Xing, X. Hu, Z. Huang, T. Hu, L. Tan, F. Li and Y. Chen, *Angew. Chem. Int. Ed. Engl.*, 2020, **59**, 16602-16608.
3. Q. Zhang, J. Duan, Q. Guo, J. Zhang, D. Zheng, F. Yi, X. Yang, Y. Duan and Q. Tang, *Angew. Chem. Int. Ed. Engl.*, 2022, **61**, e202116632.
4. C. Ge, X. Liu, Z. Yang, H. Li, W. Niu, X. Liu and Q. Dong, *Angew. Chem. Int. Ed. Engl.*, 2022, **61**, e202116602.
5. K. Zhang, Y. Deng, X. Shi, X. Li, D. Qi, B. Jiang and Y. Huang, *Angew. Chem. Int. Ed. Engl.*, 2022, **61**, e202112673.
6. T. Zheng, Q. Zhou, T. Yang, Y. Zhao, B. Fan, J. Bo, L. Fan and R. Peng, *Carbon*, 2022, **196**, 213-219.
7. Y. Lan, Y. Wang, Y. Lai, Z. Cai, M. Tao, Y. Wang, M. Li, X. Dong and Y. Song, *Nano Energy*, 2022, **100**.